Journal of Cell Science 110, 1403-1411 (1997)
Printed in Great Britain © The Company of Biologists Limited 1997
JCS3540

Crystalline mitochondrial inclusion bodies isolated from creatine depleted rat soleus muscle

Eddie O'Gorman*, Karl-Hermann Fuchs, Peter Tittmann, Heinz Gross and Theo Wallimann

Institute for Cell Biology, ETH Hönggerberg, 8093-Zürich, Switzerland

*Author for correspondence at present address: School of Biological Sciences, University of Manchester, 2.205 Stopford Building, Oxford Road, Manchester M13 9PT, UK (e-mail: eddie.ogorman@man.ac.uk)

SUMMARY

Rats were fed a 2% guanidino propionic acid diet for up to 18 weeks to induce cellular creatine depletion by inhibition of creatine uptake by this creatine analogue. Ultrastructural analysis of creatine depleted tissues showed that mitochondrial intermembrane inclusion bodies appeared in all skeletal muscles analysed, after 11 weeks of feeding. Heart had relatively few even after 18 weeks of analogue feeding and none were evident in kidney, brain or liver. These structures were strongly immuno-positive for sarcomeric mitochondrial creatine kinase and upon removal from mitochondria, the inclusion bodies were shown to diffract to a resolution of 2.5 nm. Two-dimensional image analysis and three-dimensional reconstruction revealed arrays of creatine kinase octamers with additional components between the octameric structures. The same mitochondria had a 3-fold higher extractable specific creatine kinase activity than controls. Molecular mass gel filtration of inclusion body containing mitochondrial extracts from analogue fed rat solei revealed mitochondrial creatine kinase eluting as an aggregate of an apparent molecular mass ≥2,000 kDa. Mitochondrial creatine kinase of control soleus mitochondrial extract eluted as an octamer, with a molecular mass of 340 kDa. Respiration measurements of control solei mitochondria displayed creatine mediated stimulation of oxidative phosphorylation that was absent in analogue-fed rat solei mitochondria. The latter also had 19% and 14% slower rates of state 4 and maximal state 3 respiration, respectively, than control mitochondria. These results indicate that mitochondrial creatine kinase co-crystallises with another component within the inter membrane space of select mitochondria in creatine depleted skeletal muscle, and is inactive in situ.

Key words: Mitochondrion, Creatine kinase, Crystal, Inclusion body, Oxidative phosphorylation

INTRODUCTION

Mitochondrial inclusion bodies (MIBs) are mitochondrial intermembrane electron densities which can be induced in rat skeletal muscle by creatine (Cr) depletion (DeTata et al., 1993) and induction of skeletal muscle ischemia (Hanzlikova and Schiaffino, 1977; Karpati et al., 1974). It was postulated by Hanzlikova and Schiaffino (1977) in the late seventies that a major component of these MIBs was creatine kinase (CK)(EC 2.7.3.2). Later it was found that MIBs occurred in adult rat cardiomyocytes grown in a Cr free medium, which were heavily immuno-positive for CK (Eppenberger-Erberhardt et al., 1991). Creatine kinase is expressed in a tissue specific manner and is cellularly compartmentalised (Rossi et al., 1990; Wallimann et al., 1984). Five major CK isoforms, dimeric cytosolic BB-CK (brain specific), MB-CK (cardiac muscle) and MM-CK (skeletal muscle), as well as octameric mitochondrial Mi_a-CK (ubiquitous) and sarcomeric Mi_b-CK (muscle specific), have been characterised over the past few decades (for a review see Wallimann et al., 1992). The X-ray structure at atomic resolution of chicken Mi_b-CK has recently been solved (Fritz-Wolf et al., 1996). Mi-CK is localised in the intermembrane space (IMS) of mitochondria and supplies the cytoplasm with phospho-creatine (PCr), using ATP from oxidative phosphorylation (OXPHOS), supplied by the adenine nucleotide translocator (ANT), and Cr from the cytoplasm (Saks et al., 1978). This PCr is then used by the cytosolic CK isoforms to produce ATP from ADP in areas of energy demand, i.e.:

$$PCr^{2-}+MgADP^{-}+H^{+}<\!\!-\!\!>Cr+MgATP^{2-}.$$

When rats are fed a diet of the Cr analogue guanidino propionic acid (GPA), Cr uptake by cells is competitively inhibited and the incorporated GPA is reversibly phosphorylated to phospho-GPA (GPAP) by cytosolic CK (Boehm et al., 1996). The latter acts as a high energy phosphate trap due to the fact that the K_m of CK for GPA is twice that for Cr with a far slower rate of reaction (V_{max} 1/300) compared with that for Cr (Clark et al., 1994). MIB's concommitantly arise in creatine depleted skeletal muscle (DeTata et al., 1993; Ohira et al., 1988). Mitochondria isolated from these muscles revealed a 4-fold increase in Mi_b-CK and a 3-fold increase in ANT. However, Mi_b-CK was shown to be inactive in situ by respiration analysis of Cr stimulated OXPHOS in saponin skinned fibres from 12-week GPA fed rats (O'Gorman et al., 1996).

Other major skeletal muscle adaptations to Cr depletion have been documented in the past, namely that fast glycolytic muscles increase their aerobic capacity via increased mitochondrial densities, increased respiratory chain enzyme activities (Moerland et al., 1989; Shoubridge et al., 1985) and switches from fast myosin isoform expression to the slow isoforms (Ren et al., 1995). Cr depleted skeletal muscle has also been shown to have a twofold faster poststimulation oxidative recovery than control skeletal muscle, again indicative of enhanced aerobic capacities of these cells (Moerland et al., 1989). All these reports define clear metabolic alterations due to Cr depletion of rat skeletal muscle.

MIBs are also found in enlarged muscle mitochondria of patients suffering from mitochondrial myopathies, diseases strongly associated with mutations and deletions of the mitochondrial genome (Johns, 1996; Wallace, 1992). These abnormal mitochondria are usually localised at the subsarcolemmal region of the patients' red muscle. At the light microscopical level they appear within the so-called 'ragged red fibre' area, a diagnostic marker for some mitochondrial myopathies, e.g. myoclonic epilepsy and ragged red fibres (MERRF) (Johns, 1996). These human type MIBs have also been shown to be enriched with Mi_b-CK and crystalline when laser diffraction was carried out on ultra thin sections of glutaraldehyde fixed biopsy samples (Farrants et al., 1988; Stadhouders et al., 1994). However, no one has yet been successful at removing these structures from their host mitochondria to avoid the limitations of section and chemical fixation artefact.

The aim of this study was thus to analyse the sequential appearance of MIBs in the different tissues of rats fed a 2% GPA diet for up to 18 weeks, to isolate MIBs from GPA soleus muscle and characterise them in terms of composition, structure and function.

MATERIALS AND METHODS

GPA production and animal feeding

GPA was produced according to the method of Rowley et al. (1971) and mixed at 2% (w/w) into rat food pellets by Kliba Mühlen, Switzerland. This food was administered freely to Sprague Dawley rats for up to 18 weeks.

Electron microscopy

Muscle samples were prepared for standard transmission electron microscopical analysis as described by O'Gorman et al. (1996). Suitably fixed and Lowicryl HM20 embedded solei muscle samples were used for immunogold labelling for Mi_b-CK exactly as described by Eppenberger-Erberhardt et al. (1991).

Mitochondrial cross sectional area and quantitation of mitochondria in control and GPA solei

Solei samples from control and 8 and 18 weeks of GPA fed rats were prepared for transmission EM as described above. Two blocks from each animal were used for ultra-thin sectioning, two sections from each block were used and then 5 micrographs of each (n=20) were taken of randomly chosen areas at the muscle cell periphery at a primary magnification of 6,600. The positive prints were magnified to a final magnification of 20,000, facilitating mitochondrial analysis. Micrographs were then used for quantitation and cross sectional area measurement using an Apple 2 Europlus with Graphics Tablet. Inclusion bodies were also characterised according to their intra-mitochondrial location. Type 1 inclusion bodies were those seen between the cristae membranes and Type 2 were those found between the outer and inner membranes. Very few mitochondria had both, so we calculated the percentages of mitochondria with either of the two types, as described above. For this anaylsis we used 4 randomly chosen micrographs from the previous samples of control and 8 from each of the GPA muscle samples.

Mitochondrial isolation and mitochondrial inclusion body analyses

Control and GPA rats were killed after at least 8 weeks of feeding and mitochondria were isolated from the soleus muscle of the GPA and control rats using the procedure described by O'Gorman et al. (1996). Samples (100 μl; 3 mg/ml) of isolated mitochondrial suspensions of the GPA and control rat muscle were then suspended in 200 μl 0.01% (w/w) Triton X-100 for 30 minutes with frequent vortexing; 5 μl of this solution were then applied to glow discharged carbon-coated EM copper grids, and allowed to adhere to the grids for 20 seconds. Excess solution was blotted off with filter paper and the grids were washed with 3 drops of distilled water or distilled water containing 0.01% Triton X-100. Negative staining with 2.5% acidic uranyl acetate for 10 seconds followed this and the grids were washed again as above. Grids were immediately analysed with a Philips CM 12 electron microscope. Only mitochondria from GPA soleus muscle revealed exposed MIBs, which were analysed at low (33,000) and high (60,000) magnification. Using a slow-scan CCD camera (Gatan 694) crystallinity and image quality were tested by on-line Fast Fourier Transformation, using the SW package of Digital Micrograph.

Image averaging and three-dimensional (3-D) reconstruction were carried out with the Milan image (Bittplane) processing package and executed on a Silicon Graphics Indy work station. The correlation averaging was performed according to the method of Saxton and Baumeister (1982). The resolution was assessed by the spectral-signal-to-noise-ratio criteria described by Unser et al. (1987). Tilt series reconstructions were performed also according to the method of Unser et al. (1987) and applied to a single tilt axis series of 15 averages with tilt angles uniformly distributed in the range of –60 to +60 degree.

Respiration measurements of isolated mitochondria

Respiration measurements were carried out with isolated mitochondria from control and GPA soleus muscle at 25°C, with a Cyclobios-oxygraph (Anton Paar, Innsbruck, Austria) in respiration buffer (75 mM mannitol, 250 mM sucrose, 10 mM Hepes, pH 7.4). Stimulation of OXPHOS was carried out in the presence of 5 mM succinate and 5 mM $MgCl_2$, 20 mM $Na_2H_2PO_4$ with 25 μM followed by 50 μM ADP, with and without 10 mM Cr present to analyse Mi_b-CK mediated stimulation of state 3 respiration (Saks et al., 1978).

Mitochondrial extract analyses

Mitochondria from GPA and control solei were treated in exactly the same way, as follows: mitochondrial pellets were solubilised in a 20-fold volume of water, and left to stand on ice for 20 minutes. The specimens were then exposed to 0.01% (w/w) Triton X-100 for 20 minutes, with frequent mild vortexing. Finally, alkaline $Na_2H_2PO_4.H_2O$ (pH 8.8) was added to a final concentration of 50 mM. In order to quantitatively extract Mi-CK from the mitochondria, this solution was allowed stand for 30 minutes on ice and then centrifuged for 30 minutes at 13,000 rpm at 4°C, using a Heraeus Biofuge (Schlegel et al., 1988). The supernatant was collected and the pellet washed with water before being dissolved in SDS-PAGE sample buffer (Laemmli, 1970). The extract was kept at 4°C or frozen until further analysis.

Gel filtration chromatography

A prepacked HiPrep 16/60 Sephracryl S-300 HR column was used with a FPLC system (Pharmacia) at a flow rate of 0.3 ml minute^{-1} and

calibrated with the following marker proteins (Pharmacia, elution volumes in brackets): blue dextran 2,000 kDa (39 ml), thyroglobulin 669 kDa (45 ml), ferritin 440 kDa (53 ml), aldolase 158 kDa (61 ml) and chymotrypsinogen 25 kDa (88 ml). Purified human Mi_b-CK, kindly provided by Uwe Schlattner, eluted at 55 ml (octameric form) and at 73 ml (dimeric form). The flow rate was 0.3 ml per minute using the Pharmacia LCC500 FPLC system. The running buffer always consisted of 220 mM mannitol and 10 mM Hepes buffer at pH 7.5. Samples (0.5 mg ml^{-1}) of either GPA or control extracts were loaded and absorbance read at 280 nm. Peak fractions were collected and concentrated with Centricon 30 concentrators (Amicon) and tested for CK activity using the pH stat assay (Wallimann et al., 1984).

Gel electrophoresis

12% polyacrylamide gel electrophoresis (PAGE) was carried out in the presence of SDS (Laemmli, 1970) with 10-20 μg of mitochondrial protein added per lane.

Creatine kinase and adenylate kinase specific activity

Tissue and mitochondrial extracts of GPA and control solei were analysed for creatine kinase activity in the pH stat (Wallimann et al., 1984) in 75 mM KCl, 10 mM $MgCl_2$, 0.1 mM EGTA, 1 mM β-mercaptoethanol and 4 mM ADP. The CK reaction was started upon addition of 10 mM PCr. Adenylate kinase (EC 2.7.4.3) activity was measured by a coupled enzyme assay (Bücher et al., 1964).

RESULTS

Sequential appearance of mitochondrial inclusion bodies in different tissues and in situ ultrastructural analysis

Ultrastructural analysis of soleus, diaphragm, quadriceps, heart, brain, kidney, and liver during a time course of feeding revealed a step-wise appearance of the MIBs as shown in Table 1. None were found in brain, kidey or liver. Liver served as an internal control as no CK is expressed in this tissue. It appears that those tissues expressing Mi_b-CK are the only ones capable of forming MIBs upon creatine depletion with oxidative skeletal muscle, i.e. soleus, being the first, followed by diaphragm and then the glycolytic quadriceps. Heart had only a very few present even after 18 weeks of feeding. It is already known that when metabolism is normalised, as with creatine repletion of GPA treated muscle (DeTata et al., 1993; Eppenberger-Erberhardt et al., 1991) or cessation of ischemia (Karpati et al., 1974) the inclusion bodies disappear.

Table 1. Time of consecutive appearance of MIBs in various rat tissues during a GPA feeding time course

	Days of GPA feeding					
	0	55	71	91	105	126
Soleus	–	+	+	+	+	+
Diaphragm	–	–	+	+	+	+
Quadriceps	–	–	–	+	+	+
Heart	–	–	–	–	–	+
Kidney	–	–	–	–	–	–
Liver	–	–	–	–	–	–
Brain	–	–	–	–	–	–

Overview of the appearence, as indicated by (+), of MIB containing mitochondria during a time course of feeding with GPA. The different tissues were all treated for TEM analysis as described in Materials and Methods. Note that the most oxidative muscles are the first to acquire MIB structures (soleus and then diaphragm) followed by fast glycolytic types and finally heart.

Ultra-thin sections of soleus muscle from control rat showed a normal ultrastructural appearance (Fig. 1A) whereas soleus of rats fed GPA for 8 weeks confirmed the presence of MIBs in large abnormal mitochondria located at the muscles' subsarcolemmal region (Fig. 1B). Two distinct types of MIBs were classified according to the membranes they were surrounded by; as is seen in Fig 1C, Type 1 inclusion bodies are present between the cristae membranes, with Type 2 inclusions located between the inner and outher mitochondrial membranes. Rarely were mitochondria found with both MIB types. Such a discrimination between two different inclusion body types was first described in biopsy material taken from patients suffering from mitochondrial myopathies (Farrants et al., 1988). Close examination of the cross section through the Type 1 and 2 MIB structures shown in Fig. 1C, reveals a periodic criss-cross structure strongly resembling a side view of the Mi_b-CK octamer, resolved at atomic resolution recently (Fritz-Wolf et al., 1996). The thickness of these structures was measured as approximately 10 nm which is similar to the height of the octameric Mi_b-CK crystal form (8.3 nm) (Fritz-Wolf et al., 1996).

No significant difference was found between the cross sectional area occupied by control fed soleus mitochondria and those mitochondria without MIBs in the 8- and 18-week GPA fed rat solei (Table 1). Analysis of solei mitochondria of GPA fed rats revealed no significant difference in the cross sectional area occupied by mitochondria with MIBs at 8 or 18 weeks, but this area compared to the mitochondria without MIBs was 2- to 5-fold higher, see Table 2. Out of a total of 1,523 mitochondria counted in the subsarcolemmal regions of 8-week GPA rat solei (see Materials and Methods), it was observed that a total of 25% had MIBs, 15% were Type 1, and 10% were Type 2 MIBs. These percentages did not change after 18 weeks of GPA feeding. Immunogold labelling of paraformaldehyde fixed and Lowicryl HM20 embedded soleus material of GPA fed rats revealed extensive labelling for Mi_b-CK directly over the electron dense MIB structures (Fig. 1D). On the same sections, labelling for Mi_b-CK over mitochondria without MIBs was very sparse and not much higher than background labelling. For antigenic preservation, the overall tissue and mitochondrial ultrastructure had to be compromised in favour of antigenic preservation.

Exposure of mitochondrial inclusion bodies on EM grids and image analysis

Only the GPA-soleus mitochondria treated with 0.01% Triton X-100 in H_2O revealed box-like structures lying alone in a random fashion with a layer of mitochondrial membrane (Fig. 2A). Upon close examination at a magnification of ×45,000 these structures had a regular periodic appearance and were shown to diffract, revealing their inherent crystallinity (Fig. 2B).

For the analysis of the two-dimensional (2-D) projections of MIB, the micrographs were noise-reduced by correlation averaging; 500 motifs were averaged and a lateral resolution of about 2 nm was obtained for all of the processed samples. The unit cell is rectangular with lattice constants of 128±4 by 194±8 Å (n=10). The s.d. of the constants from a single average are in the range of 5 to 10 Å indicating either fragile protein to protein contacts in the crystals, or differences occuring betweeen the two MIB types which were impossible to identify

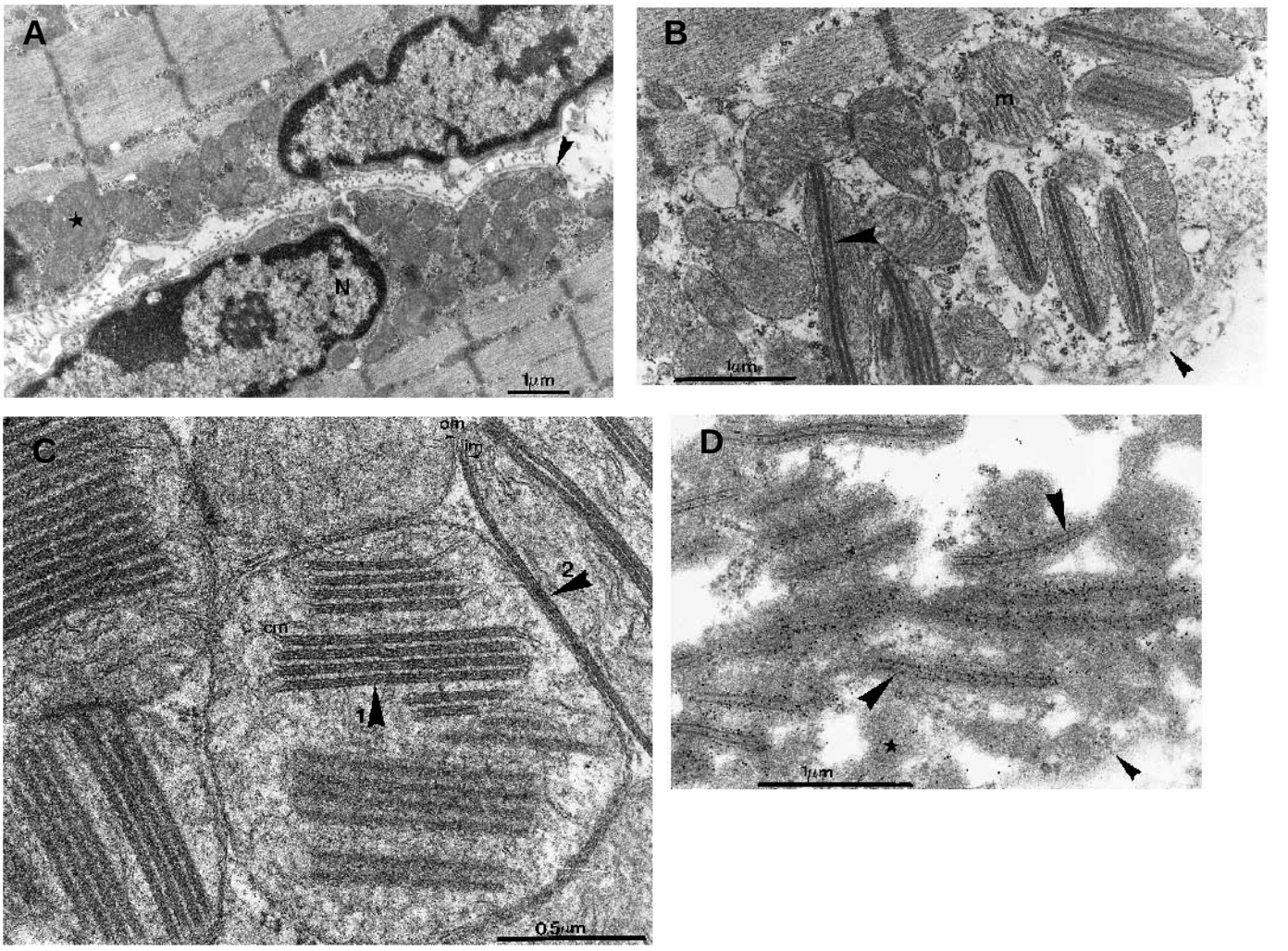

Fig. 1. Electron micrographs of glutaraldehyde fixed and osmicated soleus muscle tissue. (A) Subsarcolemmal mitochondrial populations of adjacent muscle fibres of a control soleus enveloping the nuclei of adjacent cells. Arrowhead (A and B) indicates plasma membrane. N, nucleus; star, mitochondrion. (B) Sample from a soleus of an 8-week GPA fed rat revealing enlarged mitochondria with obvious electron dense inclusion bodies between the mitochondrial cristae membranes (large arrowhead), next to normal mitochondria without inclusion bodies (M). (C) High magnification of the two different types of inclusion bodies found in separate neighbouring mitochondria in diaphragm of GPA fed rats (i.e. Types 1 and 2 as indicated with the large arrowheads and numbers 1 and 2). Note the regular periodicity of the electron dense structures. Both types of inclusion bodies are surrounded by mitochondrial membranes: Type 1 by cristae membranes (cm) and Type 2 by the inner and outer membranes (im and om, respectively). (D) Freeze substituted soleus specimen from GPA fed rat, immunolabelled for Mi_b-CK as described in Materials and Methods, using 10 nm gold-conjugated goat anti-rabbit as the secondary antibody. Note the dense labelling for Mi_b-CK over the electron dense areas of the inclusion bodies (large arrowheads). These mitochondria are also situated below the sarcolemma (small arrowhead). Star indicates mitochondria without inclusion bodies displaying immunogold labelling not higher than background.

with this method. The observed lattice dimensions give evidence that these structures represent two Mi_b-CK octamers per unit cell, represented by the rectangle in Fig. 2C.

To check for internal crystal symmetry, we ran a procedure which calculates a relative correlation coefficent between the original image and a copy rotated about the putative symmetry center. The curve obtained for the coefficients, as a function of the rotation angle and under the assumption of at most twofold symmetry, shows a significant maximum at the angle of 180 degree. This fact may be taken as a strong indication for a twofold symmetry of the unit cell in the obtained resolution range. Each unit cell encloses two identical, ring-like structures of a diameter of 100 Å and two additional smaller structures with an extension of 30 Å by 45 Å, clearly seen in the Triton X-100 washed sample (Fig. 2C). The ring-like structures resemble very closely the structure seen in 2-D crystals of Mi_b-CK octamers formed on artificial cardiolipin monolayers (Schnyder et al., 1994). In order to obtain more information on the vertical packaging, we recorded a single axis tilt series with tilting angles from –60° to +60°. Fig. 2D shows a gallery of horizontal sections at consecutive distances of 4 Å of the reconstructed 3-D map. Since the vertical resolution is only about 35 Å, minor changes in the vertical direction cannot be interpreted. The reconstruction thus shows that there is no significant structural change in the vertical direction of the crystal. This is consistent with the high symmetry and dense packaging

Table 2. Cross sectional areas of control and GPA solei mitochondria

	Number of micrographs	Inclusion body types	Number of mitochondria analysed	Mitochondrial area (μm^2)
Control	4	No MIBs	80	0.235±0.150
8 weeks GPA	8	No MIBs	160	0.267±0.153
		Type l MIBs	52	0.780±0.543
		Type ll MIBs	90	0.619±0.440
		Total	142	0.678±0.512
18 weeks GPA	8	No MIBs	160	0.255±0.163
		Type l MIBs	80	1.0032±0.622
		Type ll MIBs	80	0.76±0.641
		Total	160	0.882±0.106

Comparison of averaged cross sectional areas of subsarcolemmal mitochondria in soleus muscle of control and GPA fed rats. A significant increase in the areas of inclusion body-containing mitochondria when compared to control mitochondria within the same cells (P<0.000001) is seen. However, no significant difference in area was seen between the control soleus mitochondria and the mitochondria in GPA without inclusion bodies. The prominent standard errors in GPA samples are due to some mitochondria having lengths of up to 12 μm. The differences among different groups were tested for their significance with the non parametric rank sum test of Mann-Whitney (± s.d.).

of purified Mi_b-CK in 3-D protein crystals which makes it clear that density changes may not be expected in that resolution range (Fritz-Wolf et al., 1996). The other smaller structures evident in Fig. 2C, do not show strong density changes in the vertical direction either (Fig. 2D).

The average dimensions (length×width×height, ± s.d.) of exposed MIBs were measured as 6.6 μm (±2.5)×0.4 μm (±0.1) ×10 nm; the height corresponds to the thickness of the inclusion bodies measured in the ultra thin sections (Fig. 1C) (n=20) and would correspond to just one layer of crystallised octameric Mi_b-CK. The averaged dimensions of exposed crystals are similar to those of in situ MIBs presented in Table 2 strongly supporting the assumption that they are the same structures and mitochondrial isolation is not detrimental to overall MIB structure.

We found that isolated MIB structures were unstable in conditions of Triton X-100 concentrations higher than 0.05%, and fragmented in phosphate buffer of ≥50 mM. Our combined EM data (Figs 1, 2) show that the major component of these MIBs is octameric Mi_b-CK, co-crystallising with other unknown substructures (30 Å by 45 Å) connecting adjacent octamers (Fig. 2C,D).

Specific activities of CK and ADK in control and GPA soleus mitochondria

From Table 3 it is clear that a 3-fold increase in creatine kinase specific activity occurs in the GPA solei mitochondria, which matches closely the 4-fold increase of Mi_b-CK protein in soleus muscle mitochondria of 12-week GPA fed rats (O'Gorman et al., 1996). No difference was observed in the mitochondrial ADK activities between the two groups but 12-week GPA fed rat solei tissue extracts were shown to have double the ADK activity seen in control extracts (O'Gorman et al., 1996). Therefore it appears likely that cytoplasmic ADK is the isoform increased due to long term creatine depletion of skeletal muscle.

Table 3. Specific activities of CK and ADK in soleus of control and GPA fed rats

Control	GPA
(a) 21.0 (±1.5)	10.7 (±2.0)
(b) 2.69 (±0.5)	6.8 (±0.3)
(c) 285 mU (±7)	280 mU (±3)

(a) Specific CK activity of total soleus muscle homogenate and (b) specific Mi_b-CK activity expressed in IU corresponding to 1 μMol of PCr transphosphorylated/minute per mg of protein, as measured with the pH stat assay (Wallimann et al. (1984)), (n=5 for both sets of data). (c) ADK activity was also measured in the same mitochondrial extracts, and is expressed in mUnits (mU) of activity per mg of protein (± s.d.).

Gel filtration analysis of control and GPA mitochondrial extracts

Mitochondrial extracts were prepared so as to solubilise as little lipid from the preparation as possible, according to the standard procedure to remove Mi_b-CK from mitochondrial membranes, involving hypotonic swelling and extraction by phosphate buffer and alkaline pH (Schlegel et al., 1988). Fig. 3A reveals the total polypeptide pattern of mitochondria (mito) from control and GPA solei, the mitochondrial pellets (plt) and the extracts (ext) used for loading onto the gel filtration column in a Coomassie Blue stained 12% polyacrylamide SDS gel. No apparent difference is evident between the control and GPA mitochondrial extracts. Although the chosen conditions for gel permeation chromatography allowed further analysis of MIBs, they were not ideal for inclusion body structural preservation, since EM analysis showed that periodicity was lost and the structures were truely fragmented. On the other hand, use of lower pH, phosphate and detergent concentrations gave rise to problems of column clogging with control and GPA preparations.

However, the control mitochondrial extract with Mi_b-CK activity eluted at a peak volume of 55 ml corresponding to that of purified octameric human Mi_b-CK (Fig. 3B). By contrast, no clearly distinguishable octameric Mi_b-CK peak was observed in the GPA elution profile, the majority of Mi_b-CK eluted in the void volume peak (≥2,000 kDa), never observed with control preparations, see Fig 3B. As fractions from both peaks contained CK activity and were immuno-reactive with anti-Mi_b-CK antibodies (data not shown), it is clear that Mi_b-CK in GPA mitochondrial extracts occurs mainly in octameric aggregates (≥2,000 kDa), presumably representing MIBs. We are now isolating higher amounts of skeletal muscle mitochondria specifically for quantitative SDS-PAGE/Coomassie Blue staining and chemical-cross linking analysis, of mitochondrial IMS proteins. The cross linking study will hopefully allow us to identify the other component of the MIBs and will be aided by knowledge of the coordinates from the atomic structure of Mi_b-CK (Fritz-Wolf et al., 1996).

Respiration rates of mitochondria from control and GPA rat solei

Mitochondria were isolated from control and 8- to 10-week GPA-fed rat solei, and were analysed for respiration stimulation with 25 or 50 μM ADP, in the presence and absence of 10 mM Cr (Table 4). The control mitochondria behaved in the expected manner, in that in the presence of 10 mM Cr, 25 μM ADP was sufficient to stimulate the mitochondria to maximal state 3, as seen in the presence of 50 μM ADP or higher. However GPA

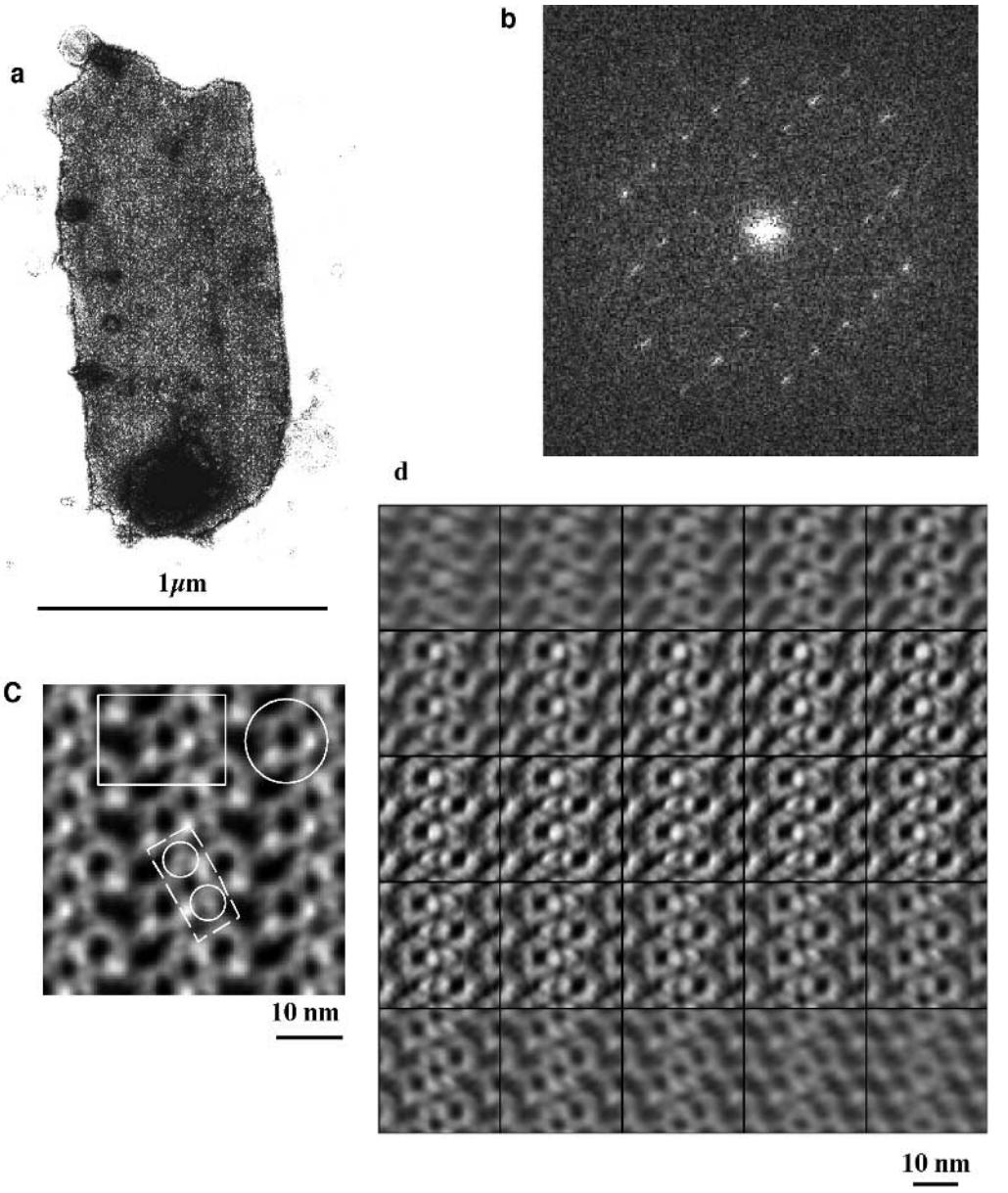

Fig. 2. Isolated MIB crystallinity, image analysis and 3-D reconstruction. (A) Low magnification EM micrograph of an isolated and exposed inclusion body. (B) A diffraction pattern of the MIB seen in (a) clearly exhibits the periodic nature of the isolated structure. (C) Average of 500 repeating motifs of a Triton X-100 washed sample. The marked structures show a unit cell (large rectangle), a single Mi_b-CK octamer (ringed) and two additional components (within small circles). (D) Horizontal sectionsof the 3-D density map obtained from a single-axis tilt series of a MIB. The distance between layers is 4 Å. The lateral resolution is 25 Å according to Unser et al. (1987). No symmetric information was exploited for the reconstruction. Changes in the density cannot be observed along the vertical axis. Parallel to the clear octameric structure of Mi_b-CK lie two substructures connecting, and of equal height to, the Mi_b-CK octamers.

solei mitochondria failed to achieve Mi_b-CK-mediated stimulation seen with 25 μM ADP and 10 mM Cr. This is similar to the finding of O'Gorman et al. (1996) who used saponin skinned soleus fibres of control and 12-week GPA fed rat solei, and found no Cr stimulation of OXPHOS in the GPA solei, in situ. Another clear difference between the control and GPA mitochondria used for respiration analysis is that state 4 and maximal state 3 respiration are slower by 19% and 14%, respectively, in GPA mitochondria compared to control values, even though the respiratory control ratios (RCR) are the same (Table 4).

DISCUSSION

Abnormal mitochondria and inclusion bodies seen in creatine deficient rat soleus

Mitochondrial inclusion bodies (MIBs) were observed in creatine deficient skeletal muscle of rats, and we have shown enrichment of Mi_b-CK within these MIBs (Fig. 1D). The differential appearance of Mi_b-CK enriched MIBs (see Results) in the different tissues described in Table 1 is likely related to the oxidative capacity of the cells. The fast type muscle (e.g. quadricep) of GPA treated rats become more metabolically oxidative with an increased mitochondrial density (Shoubridge et al., 1985; Moerland et al., 1989), increased respiratory chain activities and a switch from fast to slow myosin heavy chain isoforms (Ren et al., 1995). They are also the last skeletal muscle type to acquire MIBs (Table 1). The soleus is the best example of oxidative skeletal muscle, and is first to acquire MIBs but is known not to have remarkably enhanced oxidative capacity caused by creatine depletion, (Moerland et al., 1989). Hence the 3-fold increased Mi_b-CK (Table 3) has a similarly sized mitochondrion to that of control and crystallises out first in the mitochondria of this muscle type. This event does not

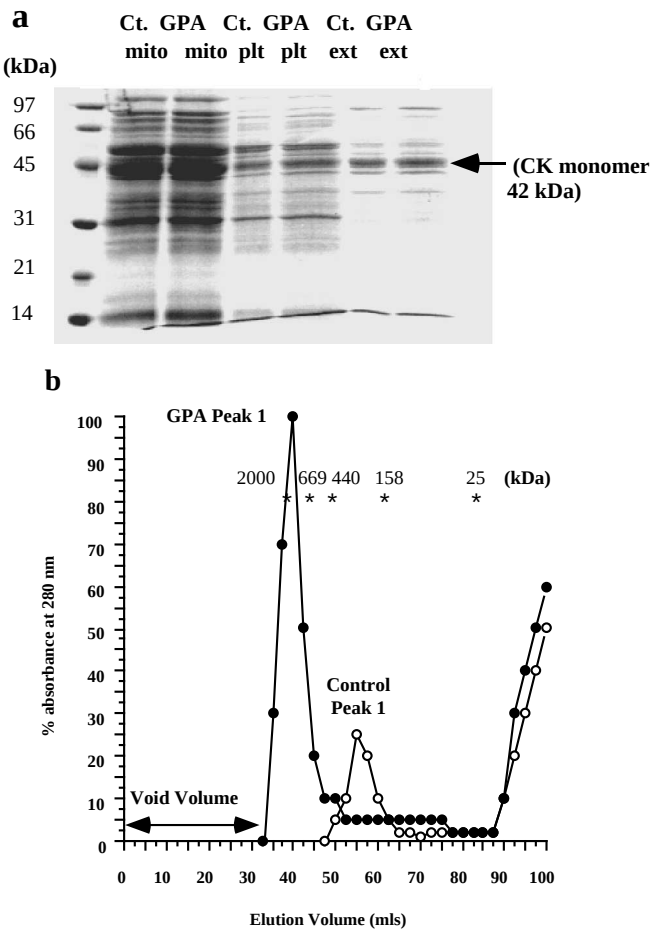

Fig. 3. (A) Coomassie Blue stained 12% SDS-PAGE gel of mitochondria from control and GPA solei, respectively (mito); mitoplast pellets (plt) and mitochondrial intermembrane extracts (ext). (B) Gel filtration protein elution profile of control and GPA mitochondrial extracts as shown in (ext) lanes of A. Stars represent the molecular mass (kDa) of the standard marker proteins used to calibrate the column (see Materials and Methods). Control Peak 1 corresponds to the position of pure octameric Mi_b-CK from control extracts, no other major protein peak was observed. If mitochondrial extracts of GPA treated animals, known to contain MIBs, were loaded onto the gel filtration column, Mi_b-CK eluted in an aggregated form of an apparent molecular mass of ≥2,000 kDa. Both control and GPA peaks had CK specific activity, however, CK yields of only 20% original activity were ever achieved with these preparations (data not shown).

occur in hearts of GPA treated rats, only after a very long period of 18 weeks of GPA feeding were MIBs observed (Table 1). The majority of Mi_b-CK in GPA soleus mitochondrial extracts occurs in a highly oligomeric (≥2,000 kDa) state as shown by gel filtration (Fig. 1D and Fig. 3B), as no true octamer peak was seen with the GPA sample. Therefore the majority of Mi_b-CK in GPA mitochondria must be within the inclusion bodies. The 3-fold increased Mi_b-CK (Table 3) mostly arises in the mitochondria containing MIBs, which represent only 25% of subsarcolemmal mitochondria. Therefore the approximate Mi_b-CK to mitochondrion ratio is closer to 12-fold higher than normal, which explains the crystallisation process in this population of subsarcolemmal mitochondria.

Table 4. Respiration analysis of isolated control and GPA solei mitochondria

	Contol soleus mitochondria		GPA soleus mitochondria	
Low state 3	(a)	(b) (10 mM Cr)	(c)	(d) (10 mM Cr)
25 μM ADP	27.4±1.1	41.0±1.5	20.5±1.5	21.5±1.4
Max state 3				
50 μM ADP	41.5±1.9	40.4±0.8	35.5±1.1	36.5±1.0
State 4				
50 μM Atr	16.5±1	17.9±0.8	13.3±0.6	13.0±1.0
Respiratory control ratios	2.5		2.6	

Respiration rates of isolated soleus mitochondria (in the isolation buffer containing 5 mM succinate, 5 mM $MgCl_2$ and 5 mM phosphate) from control and GPA fed rats were carried in the absence (a,c) and in the presence (b,d) of 10 mM Cr using an oxygen electrode (Cyclobios, Anton Parr, Austria). State 3 low and high were stimulated in the presence of 25 μM ADP and 50 μM ADP, respectively. State 4 was taken as the rate observed after the addition of 50 μM atractyloside (± s.d.). The respiratory control ratios also shown above reveal no difference between mitochondria from control and GPA fed rats. Rates are expressed as nmolO/minute per mg mitochondrial protein.

We propose that the reduced CK catalysed PCr/ATP flux causes a lower cytoplasmic ATP concentration which in turn induces overexpression of Mi_b-CK, most markedly in oxidative skeletal muscle. This hypothesis of regulation of Mi_b-CK expression by [ATP] is supported by the disappearance of these structures upon restoration of normal metabolic conditions and nutrition (DeTata et al., 1993; Eppenberger-Erberhardt et al., 1991; Karpati et al., 1974). The opposite situation exists for MM-CK, as its activity is at least 50% decreased in the GPA solei (Table 3). As we found (Table 3), there was no increase in mitochondrial ADK activity in the GPA samples, but a doubling of ADK activity was detected in GPA soleus muscle extracts (O'Gorman et al., 1996). Therefore the cytoplasmic isoform of ADK is responsible for the observed doubling of specific activity. Cytoplasmic ADK could consume liberated ADP (normally used by the cytosolic CK to form ATP from PCr), by converting it to AMP and ATP. It has already been shown that AMP deaminase mRNA is 68% lower in 6-week GPA soleus than in control (Ren and Holloszy, 1992), thus preventing a loss of adenine nucleotides via deamination of AMP produced by ADK.

These results prompt several new questions concerning the effects MIBs may have on mitochondrial protein import, especially Type 2 MIBs (Fig. 1C), such as why mitochondria with MIBs only have one inclusion type and how Mi_b-CK is so discriminatingly imported into a distinct set of subsarcolemmal mitochondria in Cr depleted soleus muscle.

Mitochondrial inclusion body structure and composition

We reveal for the first time the crystalline properties of MIBs extracted from their host mitochondria, diffracting to a resolution of 2.5 nm (Fig. 2). The averaged dimensions of the MIBs exposed on the carbon coated grids were calculated as 6.6 μm (±2.5)*0.4 μm (±0.1)*10 nm. MIBs of patients suffering from mitochondrial myopathies are also crystalline and enriched with Mi_b-CK (Stadhouders et al., 1994), but their dimensions

are quite different, human Type 1 crystals are on average 200 nm wide and 2 μm long, whereas the Type 2 crystals are more cubic in their dimensions, usually 100-300 nm in all three dimensions (Farrants et al., 1988). Furthermore there are 3 distinct populations of subsarcolemmal mitochondria in GPA soleus muscle, i.e. those without MIBs, those with Type 1 MIBs (10%) and others with Type 2 MIBs (15%). We could not distinguish between the two different MIB types with the isolation method, both of which may have different Mi_b-CK packaging. Such variations in the packaging due to different enveloping mitochondrial membranes of the two MIB types could also explain the s.d. seen with the averaged motifs, i.e. 5 to 10 Å. This would arise due to the interactions between Mi_b-CK and cardiolipin (Rojo et al., 1991; Stachowiak et al., 1996) which would be enhanced in Type 1 MIBs (surrounded by cristae membranes) and perhaps of lesser influence in the Type 2 MIBs (surrounded by both inner and outer membrane). As Mi_b-CK was shown to have an affinity for porin (Brdiczka et al., 1994), this could also influence the periodicity in the Type 2 MIBs. The detergent washed MIBs not only show a clear top view of an octameric Mi_b-CK but also of additional components between adjacent octamers (Fig. 2C). This connecting structure may explain the new unit cell size of these crystals (two Mi_b-CK octamers connected by two smaller structures (Fig. 2B), never seen with 2-D crystals of purified Mi_b-CK, (Schnyder et al., 1994). The 3-D density map also shows that the latter substructures of 30 Å by 45 Å, have height equal to that of the Mi_b-CK octamer (Fig. 2D). As no new IMS protein is co-overexpressed in these mitochondria (Fig. 3A) one could speculate that the Mi_b-CK is crystallising as an octamer-dimer unit, the dimers representing the inter-octamer bridges.

Mitochondrial function and mitochondrial myopathies

Our respiration analyses of mitochondria isolated from control and GPA solei, indicate a functionally impaired mitochondrial population in the GPA samples, i.e. a 19% and 14% decrease in state 4 and maximum state 3 rates, respectively, of oxygen consumption in the GPA solei mitochondria when compared to control (Table 4). The observed decreases of state 4 respiratory rates are close to the percentage of mitochondria with MIBs, i.e. 25% (Tables 1 and 2). Additionally, MIB-containing mitochondria in creatine deficient adult rat cardiomyocytes were shown not to be immuno-positive for aspartate amino transferase, a mitochondrial matrix marker (Eppenberger-Erberhardt et al., 1991). We assume that MIBs give rise to the slower rates of respiration due to substrate diffusion limitations through the IMS. This appears to be the case for Mi_b-CK within the MIBs as in organelles the enzyme appears inactive (Table 4), as no effect on state 3 respiration was seen in the presence of Cr. Upon extraction, leading to MIB fragmentation, a 3-fold increase in CK specific activity is observed (Table 3). It may be that the inter-octamer connecting structure may seriously impede Cr entry into the Mi_b-CK active sites. We can exclude the possibility that this high activity is due to activation of oxidised CK in the reducing conditions of the pH-stat mixture (including 1 mM β-mercaptoethanol) since the time course of activity was linear and not exponential, as would be observed in the case of re-activation. As overall succinate dehydrogenase activities in soleus muscle remains the same or even increases (Shoubridge et al., 1985; Moerland et al., 1989) subtle differences in such activities may not be readily seen when carried out with tissue extracts. Moerland et al. (1989) reported that Cr depleted fast type muscle (extensor digitorum longus) had only a 30-55% increase in aerobic capacity but a 3.5-fold increased poststimulation of oxidative metabolism recovery rate. These results indicate that either an increased mitochondrial synthesis occurs to replace the functionally impaired MIB containing mitochondria, or the mitochondria of GPA skeletal muscle have increased capacity for ATP production as has been indicated by Freyssenet et al. (1994) and O'Gorman et al. (1996), as a compensation to Cr depletion.

A reduced function of Mi_b-CK in skeletal muscles of mitochondrial myopathy patients is suggested by the significantly longer recovery period of PCr in their skeletal muscle (58-71 seconds) when compared to control patients (17-35 seconds) (Taylor and Radda, 1994). Another recent report supports the concept of CK involvement in some symptoms of at least one mitochondrial myopathy patient, as Cr supplementation increased his exercise tolerance 3-fold (Hagenfeldt et al., 1994). Creatine supplementation may help to dissociate MIBs, if ragged red fibres are present, into functional Mi_b-CK octamers, and normalise PCr supply to the muscle cytoplasm.

We propose that this method of Cr depletion offers a relatively easy way to study the control mechanism of Mi_b-CK expression (Klein et al., 1991) and protein import into skeletal muscle mitochondria, of which little is known (Attardi and Schatz, 1988). A recent report quantifies a definite difference between protein import rates of subsarcolemmal and intermyofibrillar mitochondria, which may have relevance to this particular study (Takahashi and Hood, 1996). The result that Mi_b-CK seems to co-crystallise with an unidentified structure is a new and interesting one and may give insight into Mi_b-CK's interactions with proteins in the IMS.

Uwe Schlattner is acknowledged for use of his human Mi_b-CK in calibrating the gel filtration column. We gratefully appreciate all the help given to us by Prof. Brdiczka, his group members and especially Dr Thomas Schnyder for introducing one of us (E.O'G.) during the early phase of this project to the preparative methods of the inclusions for EM. Many thanks are also offered to Dr Inka Riesinger for supplying us with some excellent electron micrographs of rat skeletal muscle. This work was funded by the Swiss Foundation for Research on Muscle Diseases (to T.W. and E.O'G.) and by SYNERGEN AG, CH-6330 Cham, Zug, Switzerland (to T.W.).

REFERENCES

Attardi, G. and Shatz, G. (1988). Biogenesis of mitochondria. *Annu. Rev. Cell Biol.* **4**, 289-333.

Brdiczka, D., Kaldis, P. and Wallimann, T. (1994). In vitro complex formation between the octamer of mitochondrial creatine kinase and porin. *J. Biol. Chem.* **269**, 27640-27644.

Boehm, E. A., Radda, G. K., Tomlin, H. and Clark, J. F. (1996). The utilization of creatine and its analogues by cytosolic and mitochondrial creatine kinase. *Biochim. Biophys. Acta.* **1274**, 119-128.

Bücher, T., Luh, W. and Pette, D. (1964). Einfach und zusammengestze optische Tests mit Pyridininucleotiden. In *Hoppe-Seyler and Thierfelder Handbuch der Physiologisch- und Pathologisch-chemischen Annalyse* (ed. K. Lang and E. Lehrartz), vol. VIA, pp. 293-339. Springer: Berlin, Goettingen, Heidelberg.

Clark, J. F., Khuchua, Z., Kuznetzov, A. V., Vasssil'eva, E., Boehm, E., Radda, G. K. and Saks, V. (1994). Actions of the creatine analogue β-

guanidinopropionic acid on rat heart mitochondria. *Biochem. J.* **300**, 211-216.

DeTata, V., Cavallini, G., Pollera, M., Gori, Z. and Bergamini, E. (1993). The induction of mitochondrial myopathy in the rat by feeding beta-guanidinopropionic acid and the reversibility of the induced lesions: a biochemical and ultrastructural investigation. *Int. J. Exp. Path.* **74**, 501-509.

Eppenberger-Erberhardt, M., Riesinger, I., Messerli, M., Schwarb, P., Müller, M., Eppenberger, H. M. and Wallimann, T. (1991). Adult rat cardiomyocytes cultured in creatine-deficient medium display large mitochondria with paracrystalline inclusions, enriched for creatine kinase. *J. Cell Biol.* **113**, 289-300.

Farrants, G. W., Hovmöller, S. and Stadhouders, A. D. M. (1988). Two types of mitochondrial crystals in diseased human skeletal muscle fibres. *Muscle & Nerve*. **11**, 45-55.

Freyssenet, D., Berthon, P., Geyssant, A. and Denis, C. (1994). ATP synthesis kinetic properties of mitochondria isolated from the rat extensor digitorum longus muscle depleted of creatine with beta guanidinopropionic acid. *Biochim. Biophys. Acta*. **1186**, 232-236.

Fritz-Wolf, K., Schnyder, T., Wallimann, T. and Kabsch, W. (1996). Structure of mitochondrial creatine kinase. *Nature* **381**, 341-345.

Hagenfeldt, L., Döbeln, U., Solders, G. and Kaijser, L. (1994). Creatine treatment in MELAS. *Muscle & Nerve* **17**, 1238.

Hanzlikova, V. and Schiaffino, S. (1977). Mitochondrial changes in ischemic skeletal muscle. *J. Ultrastuct. Res.* **60**, 121-133.

Johns, D. R. (1996). The other human genome: Mitochondrial DNA and disease. *Nature Med.* **2**, 1065-1068.

Karpati, G., Carpenter S., Melmed, C. and Eisen, A. A. (1974). Experimental ischemic myopathy. *J. Neurol. Sci.* **23**, 129-161.

Klein, S. C., Haas, R. C., Perrymann, M. B., Billadello, J. J. and Strauss, A. W. (1991). Regulatory element analysis and structural characterization of the human sarcomeric mitochondrial creatine kinase gene. *J. Biol. Chem.* **266**, 18058-18065.

Laemmli, U. K. (1970). Cleavage of structural proteins during the assembly of the head of bacteriophage T4. *Nature* **227**, 1133-1142.

Moerland, T. S., Wolf, N. G. and Kushmerick, M. J. (1989). Administration of a creatine analogue induces myosin transitions in muscle. *Am. J. Physiol.* **257**, C810-C816.

O'Gorman, E., Beutner, G., Wallimann, T. and Brdiczka, D. (1996). Differential effects of creatine depletion on the regulation of enzyme activities and on creatine-stimulated mitochondrial respiration in skeletal muscle, heart and brain. *Biochim. Biophys. Acta.* **1276**, 161-170.

Ohira, Y., Kanzaki, M. and Chen, C. S. (1988). Intramitochondrial inclusions caused by depletion of creatine in rat skeletal muscles. *Jap. J. Physiol.* **38**, 159-166.

Ren, J. M. and Holloszy, J. O. (1992). Adaptation of rat skeletal muscle to creatine depletion: AMP deaminase and AMP deamination. *J. Appl. Physiol.* **73**, 2713-2716.

Ren, J. M., Ohira, Y., Holloszy, J. O., Hämäläinen, N., Traub, I. and Pette, D. (1995). Effects of β-guanidinopropionic acid-feeding on the patterns of myosin isoforms in rat fast-twitch muscle. *Eur. J. Physiol.* **430**, 389-393.

Rojo, M., Hovius, H., Demel, R. A., Nicolay, K. and Wallimann, T. (1991). Mitochondrial creatine kinase mediates contact formation between mitochondrial membranes. *J. Biol. Chem.* **226**, 20290-20295.

Rowley, G. L., Greenleaf, A. L. and Kenyon, G. L. (1971). On the specificity of creatine kinase. New glycocyamines and glycocyamine analogs related to creatine. *J. Am. Chem. Soc.* **93**, 5542-5551.

Rossi, A. M., Eppenberger, H. M., Volpe, P., Cotrufo, R. and Wallimann, T. (1990). Muscle-type MM creatine kinase is specifically bound to sarcoplasmic reticulum and can support Ca^{2+} uptake and regulate local ATP/ADP ratios. *J. Biol. Chem.* **265**, 5258-5266.

Saks, V. A., Rosenshtraukh, L. V., Smirnov, N. and Chazov, E. I. (1978). Role of creatine phosphokinase in cellular function and metabolism. *Can. J. Physiol. Pharmacol*. **56**, 691-706.

Saxton, W. O. and Baumeister, W. (1982). Three-dimensional reconstruction of imperfect two-dimensional crystals. *Ultramicroscopy* **13**, 57-70.

Schlegel, J., Zurbriggen, B., Wegmann, G., Wyss, M., Eppenberger, H. M. and Wallimann, T. (1988). Isolation of two interconvertible mitochondrial creatine kinase forms, dimeric and octameric mitochondrial creatine kinase: characterisation, localisation, and structure-function relationships. *J. Biol. Chem.* **262**, 16942-16593.

Schnyder, T., Cyrklaff, M., Fuchs, K. H. and Wallimann, T. (1994). Crystallisation of mitochondrial creatine kinase on negatively charged lipid layers. *J. Struct. Biol.* **112**, 136-147.

Shoubridge, E. A., Challiss, R. A. J., Hayes, D. J. and Radda G. K. (1985). Biochemical adaptation in the skeletal muscle of rats depleted of creatine with the substrate analogue beta-guanidinopropionic acid. *Biochem. J.* **232**, 125-131.

Stachowiak, O., Dolder, M. and Wallimann, T. (1996). Membrane-binding and lipid vesicle cross-linking kinetics of the creatine kinase octamer. *Biochemistry* **35**, 15522-15528.

Stadhouders, A. M., Jap, P., Winkler, H. P., Eppenberger, H. M. and Wallimann T. (1994). Mitochondrial creatine kinase: A major constituent of pathological inclusions seen in mitochondrial myopathies. *Proc. Nat. Acad. Sci. USA* **91**, 5089-5093.

Takahashi, M. and Hood, D. A. (1996). Protein import into subsarcolemmal and intermyofibrillar skeletal muscle mitochondria. *J. Biol. Chem.* **271**, 27285-27291.

Taylor, D. J. and Radda G. K. (1994). Mitochondrial disease: noninvasive techniques. In *Current Topics in Bioenergetics 17: Molecular Basis of Mitochondrial Pathology* (ed. C. P. Lee), pp. 99-123. Academic Press, London.

Unser, M., Trus, B. L. and Steven, C. (1987). A new resolution criterion based on the spectral signal to noise ratios. *Ultramicroscopy* **23**, 39-41.

Wallace, D. C. (1992). Diseases of mitochondrial genes. *Annu. Rev. Biochem.* **61**, 1175-1212.

Wallimann, T., Schlösser, T. and Eppenberger, H. M. (1984). Function of M-line bound creatine kinase as intramyofibrillar ATP regenerator at the receiving end of the phosphorylcreatine shuttle in muscle. *J. Biol. Chem.* **209**, 5238-5246.

Wallimann, T., Wyss, M., Brdiczka, D. and Nicolay, K. (1992). Intracellular compartmentation, structure and function of creatine kinase isoenzymes in tissues with high and fluctuating energy demands: the 'phosphocreatine circuit' for cellular energy homeostasis. *Biochem. J.* **281**, 21-40.

(Received 5 February 1997 – Accepted 11 April 1997)